

DISCOVERY OF LOW DM FAST RADIO TRANSIENTS: GEMINGA PULSAR CAUGHT IN THE ACT

YOGESH MAAN¹

National Centre for Radio Astrophysics, Pune 411007, India

ABSTRACT

We report discovery of several energetic radio bursts at 34 MHz, using the Gauribidanur radio telescope. The radio bursts exhibit two important properties associated with the propagation of astronomical signals through the interstellar medium: (i) frequency dependent dispersive delays across the observing bandwidth, and (ii) Faraday rotation of the plane of linear polarization. These bursts sample a range of dispersion measures (DM; $1.4\text{--}3.6\text{ pc cm}^{-3}$), and show DM-variation at timescales of the order of a minute. Using groups of bursts having a consistent DM, we show that the bursts have originated from the *radio-quiet* gamma-ray pulsar Geminga. Detection of these bursts supports the existence of occasional radio emission from Geminga. The rare occurrence of these bursts, and the short timescale variation in their DM (if really caused by the intervening medium or the pulsar magnetosphere), might provide clues as to why the pulsar has not been detected in earlier sensitive searches. We present details of the observations and search procedure used to discover these bursts, a detailed analysis of their properties, and evidences of these bursts being associated with Geminga pulsar, and discuss briefly the possible emission mechanism of these bursts.

Subject headings: Pulsars: General — Pulsars: Individual (J0633+1746, J0633+0632) — ISM: general — polarization — methods: data analysis — radiation mechanisms: general

1. INTRODUCTION

Detection of fast radio transients has been key to several important discoveries. Discovery of several pulsars, including the first ever discovered pulsar B1919+21 (Hewish et al. 1968), has been made through the detection of their single pulses. The Crab pulsar was also discovered through its giant pulses (Staelin & Reifenstein 1968). Discovery of rotating radio transients (RRATs; McLaughlin et al. 2006) — a category of pulsars that are highly intermittent in their emission — would not have been possible without a systematic search for transients. More recently, a new class of bright dispersed pulses, called fast radio bursts (FRBs), has been discovered (Lorimer et al. 2007; Keane et al. 2012; Thornton et al. 2013). Most of the FRBs have been discovered far from the Galactic plane, and yet at anomalously high dispersion measures (DMs; in the range $375\text{--}1630\text{ pc cm}^{-3}$). The excess in DM is assumed to be contributed by the extra-galactic medium, and hence, most of the FRBs are considered to be of extra-galactic origin. The narrow pulse-widths (of the order of a few milliseconds) and high brightness temperatures of the FRBs indicate towards coherent emission processes. Although several possible progenitors have been proposed (e.g., merging binary white dwarf systems (Kashiyama et al. 2013), collapsing supramassive neutron stars (Falcke & Rezzolla 2014), hyperflares from extra-galactic magnetars (Popov & Postnov 2007), binary neutron star mergers (Totani 2013), synchrotron maser emission from relativistic, magnetized shocks (Lyubarsky 2014), collisions between axion stars and neutron stars (Iwazaki 2015), radio waves from pulsar companions (Mottez & Zarka 2014)), the exact physical nature of the FRBs still remains unknown and awaits

for further clues from future detections.

The aforementioned discoveries, especially that of the FRBs, have enormously boosted the searches for fast transients across a large span of radio wavelengths. However, such explorations are still very limited in the low frequency part of the radio spectrum ($\lesssim 100\text{ MHz}$). Some of the transient sources at these wavelengths include sporadic emission from known and unknown pulsars and RRATs, and radio flares from active stars and planets (like Jovian bursts). Recent detection of transient radio signals from the gamma-ray pulsar J1732–3131 (Maan et al. 2012) demonstrated the potential scope of low frequency searches in detecting the low frequency counterparts of *radio-quiet* gamma-ray pulsars. The discovery of several bright dispersed pulses presented in this article are most likely associated with the first ever discovered radio-quiet gamma-ray pulsar J0633+1746 — also known as Geminga pulsar.

The search for continuum as well as pulsed radio emission from Geminga has a long history, with some claimed detections as well as very sensitive upper flux density limits on pulsed emission. Although three research groups from the Pushchino radio astronomy observatory claimed low significance ($< 10\sigma$) detections of pulsed radio emission from this pulsar (with flux densities in the range $30\text{--}100\text{ mJy}$ at 102.5 MHz ; Malofeev & Malov 1997; Kuz'min & Losovskii 1997; Shitov & Pugachev 1998) at a DM of about 3 pc cm^{-3} , several other sensitive searches, before as well as after the above claimed detections, have remained unsuccessful (e.g., Seiradakis 1992; Ramachandran et al. 1998; Ershov 2007; Coenen 2013; Maan & Aswathappa 2014). A possible detection of the pulsar was also reported using the Rajkot radio telescope (India) at 103 MHz (Vats et al. 1999). More recently, Malov et al. (2015) have presented further, albeit still low-significance, detections of radio pulses from this pulsar at 42 , 60 and 111 MHz . Given the low significance

ymaan@ncra.tifr.res.in

¹ Raman Research Institute, Bangalore 560080, India

of all the claimed detections so far, credibility of these detections have been questioned against the sensitive upper limits. Detection of strong pulses presented in this paper will hopefully provide clues why this pulsar has been detectable only occasionally.

We describe our observations and search procedure in Section 2, present the discovery and properties of several radio bursts in Section 3, discuss possible source of the bursts and present their most likely association with Geminga pulsar in Section 4, followed by a summary of the findings in Section 5.

2. OBSERVATIONS AND SEARCH PROCEDURE

The east-west (EW) arm of the Gauribidanur radio telescope (Deshpande, Shevgaonkar, & Sastry 1989) was used to observe the gamma-ray pulsars J0633+1746 and J0633+0632 at 34 MHz, with a bandwidth of 1.53 MHz. The beamwidths of the EW array are $21'$ and $25^\circ \times \text{sec}$ (zenith angle) in right ascension (RA) and declination (Dec), respectively. Sky position of the two pulsars differ by approximately $13''$ and 11.3° in RA and Dec, respectively. Given the above telescope beamwidth, both the pulsars could be observed simultaneously in a single pointing². The effective collecting area offered by the EW arm is 12000 m^2 at the instrumental zenith ($+14^\circ.1$ declination). A total of 130 observing sessions, each typically 30 minutes long, were conducted between June 23, 2012 and April 18, 2013. Severe radio frequency interference (RFI) made 31 of these sessions completely unusable, and results from the remaining 99 sessions are presented below. First 45 observing sessions could use only 80% of the total collecting area since 10% of the dipoles at each of the two far ends of the arm had some technical problem. Results of deep searches for the periodic radio signals from both the pulsars, using these 45 observing sessions, were reported in Maan & Aswathappa (2014). Observations towards several radio-quiet gamma-ray pulsars were also reported by Maan & Aswathappa (2014), which serve as blank sky observations for the findings presented below. Additionally, at least one of the two control pulsars — B0834+06 and B1919+21 — was observed on the days when the target source observations were conducted.

During each of the observing sessions, Nyquist sampled raw voltage sequence is recorded with 2-bit, 4-level quantization. In the off-line processing, the voltage time sequences are converted to filterbank format with desired spectral and temporal resolutions. To identify the parts of data that are contaminated by RFI, robust mean and standard deviation are calculated separately in the time and frequency domains. Appropriate threshold in signal-to-noise ratio (typically around 10) is used to identify the RFI contaminated spectral channels and time samples separately. Identifying the bad frequency channels involves comparing the above statistical quantities with those of a smoothed, fitted radio spectrum (reflecting largely the instrumental response, i.e., the filter bandshape). The potential RFI contaminated time samples

are excluded while identifying the bad frequency channels and vice-versa. Note that the above threshold based algorithm works well even in the presence of pulsed radio signals from a pulsar, since (1) the intrinsic spectra of pulsars are smooth, and (2) the time-smearing of pulsed signals due to dispersion in the interstellar medium is quite significant, especially at such low frequencies. The frequency channels and time samples identified as RFI contaminated are excluded from any further processing.

The filterbank data, having typically 512 spectral channels at a resolution of $\sim 1 \text{ ms}$, are searched for fast transients in the DM range of $0\text{--}50 \text{ pc cm}^{-3}$. Briefly, the search for fast transients involves dedispersing the filterbank data at several optimally spaced trial DMs, and searching the individual dedispersed time series for candidate pulses above a specified detection threshold. For an optimum detection, a search across the pulsewidth is also conducted in each of the dedispersed time series. For more details of the search procedure as well as those of the acquisition setup, the Gauribidanur radio telescope, and the pre-search data processing, we refer the reader to Maan et al. (2012) and Maan (2014); Maan & Aswathappa (2014).

3. DISCOVERY OF RADIO TRANSIENTS AND THEIR PROPERTIES

Our search for fast radio transients resulted in detection of bright radio pulses from the observing sessions conducted on July 13, 2012 and July 15, 2012 (here onwards session A and B, respectively). A very strong, dispersed pulse with a signal-to-noise ratio (S/N) more than 200, was discovered at a DM of $\sim 2.1 \text{ pc cm}^{-3}$ in session A. Both the sessions A and B were conducted in the day time, and suffered heavily from RFI. Although prominent RFI contaminated spectral channels as well as time samples were identified and excluded, several low-level RFI intervals escaped our threshold based RFI-identification algorithm. These remnant RFI intervals reduced the sensitivity towards faint transient events. Dynamic spectra of session A and B were manually inspected to identify the remnant potential RFI intervals. In total, about 25% of the time-samples were flagged as RFI-contaminated. The flagged samples were excluded from any further processing, including the repeated transient search. The repeated search uncovered several other dispersed pulses. A couple of bright pulses discovered in session A are shown in Figure 1. All the bursts discovered in session A and B are listed in Table 1.

3.1. Dispersion Measures of the Bursts

Propagation of a radio signal through the ionized interstellar medium (ISM) introduces frequency dependent delay in its arrival time. Considering the ISM to be cold plasma comprised of free electrons, the delay (Δt) has a power law dependence on frequency (ν) and the dispersion measure (DM; the integrated column density of free electrons along the line of sight): $\Delta t \propto \text{DM} \nu^{-2}$. As shown by the reference lines indicating the expected quadratic delay as a function of frequency in Figure 1, the radio bursts closely follow the expected cold plasma dispersion relationship. A quantitative fit of the observed frequency dependence has not been possible due to presence of a mixed variety of spectral features (some of

² The position coordinates ([RA,Dec]) of the pulsars J0633+0632 and J0633+1746, when precessed to the observing epoch (2012–2013), are $[06:34:26, 6.5^\circ]$ and $[06:34:38, 17.8^\circ]$ respectively. Both the pulsars were observed simultaneously by pointing towards the direction $[06:34:26, 10^\circ]$.

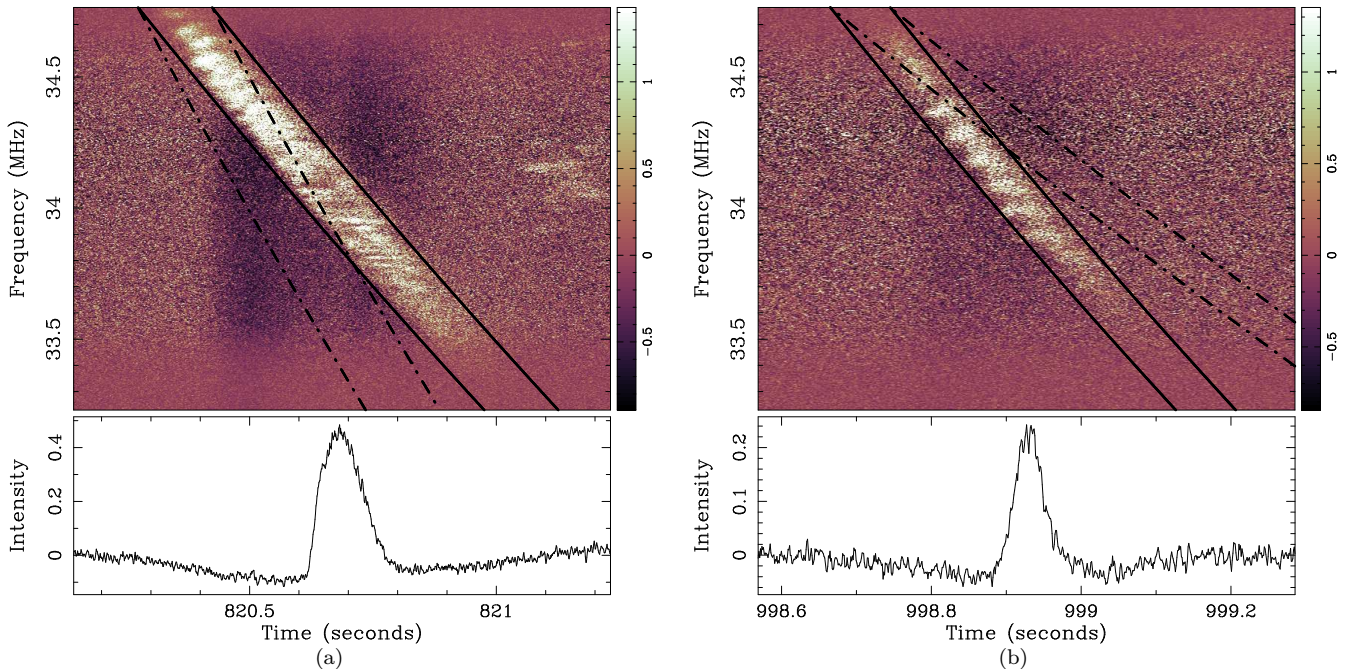


FIG. 1.— *Two bright radio bursts discovered in session A:* In each of the subfigures (a) and (b), the upper panel shows a part of the dynamic spectrum centered at the position of the burst. The pairs of continuous slanted lines that bound the pulse, show the expected quadratic behavior for the cold-plasma dispersion relation, corresponding to the respective best-estimated DMs — 2.16 pc cm^{-3} and 1.42 pc cm^{-3} for the bursts in subfigures (a) and (b), respectively. To demonstrate the difference in the two DM values, the dash-dot-dashed lines in subfigure (a) shows the dispersion relation corresponding to the DM of the burst in (b), and vice-versa. The lower panels show the total intensity as a function of time measured from the start of the observation, after dispersive delays are corrected using the corresponding best-estimated DMs (for a reference frequency of 34 MHz). The intensity in both the panels is in units of system temperature.

which we use to deduce polarization properties of the bursts as explained below). The estimated DMs of all the radio bursts sample a range of $1.4\text{--}3.6 \text{ pc cm}^{-3}$ (see Table 1). The uncertainty in DM is measured by examining the significance of the dedispersed pulse as a function of trial DM, and corresponds to a change which degrades the peak amplitude of the pulse by 1σ . The measured uncertainties have been successfully cross-checked against the theoretical predictions (using equation 12 of Cordes & McLaughlin 2003). The significant difference in the DMs of different bursts is apparent in Figure 1, wherein the quadratic dispersion relation curves corresponding to DMs of two pulses are shown together.

3.2. Deducing Linear Polarization Properties and Faraday Rotation from Spectral Intensity Modulation

Several of the radio bursts exhibit a variety of spectral structures, sometimes at frequency scales as small as a few tens of kHz (see e.g., Figure 1(a)). These spectral features may have been contributed by, either individually or a combination of, the intrinsic spectrum of the bursts and the propagation effects. The narrow bursts shown in Figure 1 extend nearly throughout the observed bandwidth. Although intrinsically narrow emission bandwidth is possible, it is unlikely for an astronomical source to have narrow, systematic spectral features within an intrinsically (relatively) wideband emission. The relevant propagation effects include interstellar scintillation and the Faraday rotation in the magneto-ionic medium. The scintillation bandwidth towards the direction of our observation, estimated using the NE2001

model (Cordes & Lazio 2002), varies from a few kHz to a few tens of kHz for the DM range of $1.4\text{--}3.6 \text{ pc cm}^{-3}$, and might explain some of the observed spectral features.

Faraday rotation in the intervening magneto-ionic medium rotates the plane of the linear polarization. Rotation Measure (RM) — the line-of-sight component of the intervening magnetic field weighted by the electron density and integrated over the distance — characterizes the amount of frequency-dependent rotation: $\Delta\theta = \text{RM}\lambda^2$, where λ is the wavelength of observation. Note that the Gauribidanur radio telescope is receptive to only a single linear polarization (in east-west direction). For such a telescope, the differential Faraday rotation of the linearly polarized component of the signal results in spectral intensity modulation within the observation bandwidth (see, e.g., Ramkumar & Deshpande 1999). The observed spectral intensity modulation can be exploited to estimate RM, and study the linear polarization properties (i.e., degree of polarization and the polarization position angle) of the signal. For this purpose, we have used an approach similar to the “auto-correlation domain approach” described by Ramkumar & Deshpande (1999). To estimate RM, we take the radio frequency spectrum at each of the time samples within the pulse, transform the frequency values corresponding to different spectral channels to square of their respective wavelengths (λ), and take a discrete Fourier transform of the spectrum in the λ^2 -domain. The Fourier conjugate of λ^2 is directly proportional to RM, and hence the above discrete Fourier transform provides linearly polarized power as a function of RM. In this ‘Faraday spectrum’, the spectral modulation due to the Faraday rotation would

TABLE 1

PROPERTIES OF ALL THE RADIO BURSTS DISCOVERED IN SESSION A AND B. THE ARRIVAL TIMES (PULSE-CENTROIDS) ARE GIVEN WITH RESPECT TO THE START OF OBSERVATIONS, PULSE-WIDTHS ARE ROUNDED-OFF TO NEAREST MULTIPLE OF 5, AND PULSE-ENERGIES ARE ROUNDED-OFF TO NEAREST MULTIPLE OF 100. THE PULSE-ENERGIES INSIDE SQUARE BRACKETS ASSUME THE GEMINGA PULSAR TO BE THE SOURCE OF RADIO BURSTS, WHILE THOSE OUTSIDE THE BRACKETS ASSUME THE SOURCE TO BE AT THE TELESCOPE POINTING CENTER. *Absolute* VALUES OF RM ARE GIVEN, SINCE THE SIGN CAN NOT BE INFERRED.

Sr. No.	Time of arrival (seconds)	Pulse width (ms)	Pulse Energy (Jy.ms)	Dispersion Measure (pc cm ⁻³)	Rotation Measure [†] (Rad. m ⁻²)
<i>Session A (MJD at start of observation: 56121.247581019)</i>					
1	820.69 ± 0.03	110	403000	[556900]	—
2	823.53 ± 0.02	75	174000	[240500]	9.4 ± 0.8
3	824.43 ± 0.03	85	159700	[220700]	12.6 ± 2.8 [‡]
4	944.11 ± 0.03	140	81000	[111900]	—
5	998.93 ± 0.02	55	89600	[123800]	7.3 ± 0.4
6	1000.41 ± 0.02	90	60300	[83400]	7.0 ± 0.7
7	1157.89 ± 0.03	95	22200	[30600]	6.3 ± 1.1
8	1169.80 ± 0.03	180	58600	[81000]	—
9	1172.50 ± 0.01	50	21600	[29800]	—
10	1176.86 ± 0.01	35	26600	[36800]	10.6 ± 1.3
11	1177.08 ± 0.01	30	26400	[36400]	10.7 ± 1.1
12	1186.41 ± 0.04	170	18500	[25500]	—
13	1187.39 ± 0.02	195	28300	[39000]	—
<i>Session B (MJD at start of observation: 56123.232627315)</i>					
14	713.10 ± 0.04	130	57100	[79000]	—
15	1345.99 ± 0.07	270	91300	[126200]	—
16	1518.90 ± 0.05	150	106600	[147300]	—

[†] Power in some of the bursts do not extend throughout the full observed bandwidth of 1.5 MHz, and hence correspondingly limited parts of the bandwidth were used in the RM-synthesis of these bursts. For bursts 3, 6, 7, 10 and 11, *effective* bandwidths used to estimate RM are 0.3, 1.0, 0.6, 0.5 and 0.6 MHz, respectively.

[‡] The Faraday spectrum of this burst is not well resolved, and RM corresponding to the brightest component is provided here.

appear as a narrow feature convolved with the Fourier transform of the filter response (i.e., bandshape). Note that in the absence of prior knowledge of the polarization position angle (PPA) sweep across the pulse, the above process needs to be performed separately on spectra corresponding to the individual samples, amounting to a *time-resolved RM synthesis*. However, in this method, the RM estimation is limited by S/N of individual samples. A more sensitive estimate of RM is obtained by incoherently adding the spectral modulation power in various samples, i.e., by taking a weighted or simple average of the Faraday amplitude spectra across the pulse. After estimating the RM, fractional linear polarization and PPA can be estimated across the pulse by using the amplitude and phase of the corresponding feature in the Faraday spectra.

The above method of deducing RM and linear polarization properties was successfully tested using simulated data as well as known pulsars observed using Gauribidanur and Ooty radio telescopes (at 34 and 326.5 MHz, respectively). At 34 MHz, RM as well as linear polarization properties of B0950+08 were deduced using filterbank data (with 512 channels across 1.53 MHz bandwidth and a time resolution of 1.66 ms) from a 30 minutes long observation. The deduced RM of 2.8 ± 0.4 rad m⁻² and percentage linear polarization of about 60% are consistent with the earlier published values of 2.15 rad m⁻² and 73.9%, respectively (at 150 MHz; Noutsos et al. 2015). At 326.5 MHz, an approximately 5 minutes long observation of the bright pulsar B0740–28 using the new software back-end (Naidu et al. 2015) of the Ooty radio telescope was

utilized. Using the data in filterbank format with time and frequency resolutions of about 1 ms and 15.6 kHz, respectively, the deduced RM (155 ± 5 rad m⁻²) and percentage linear polarization (about 92%) of B0740–28 are consistent with the earlier reported values at 435 MHz (150.4 rad m⁻² and 83%, respectively; Gould & Lyne 1998; Manchester, Han & Qiao 1998). The deduced PPA sweeps of the two pulsars were also found to be consistent with those reported at nearby frequencies.

In Figure 2(a), a time-resolved RM synthesis performed on the burst in Figure 1(b) is shown. Using the average Faraday amplitude spectrum, RM for this pulse is estimated to be 7.3 ± 0.4 rad m⁻². Having estimated the RM, fractional linear polarization and PPA can be estimated across the pulse by using the amplitude and phase of the corresponding feature in the Faraday spectra. The linear polarization properties of the burst obtained in this way are shown in Figure 2(b).

The pattern of spectral features in the observed dynamic spectra of various bursts is likely to be a superposition of the spectral intensity modulation due to Faraday rotation and random modulations due to interstellar scintillation on the scale of scintillation bandwidth. Consequently, in the Faraday spectrum, the feature due to Faraday rotation is also convolved with the Fourier transform of the modulations due to scintillation. The random modulation are smeared out if the signal can be averaged over spans much longer than the scintillation time. In our case of RM synthesis using single pulses, this effect is more relevant and generally increases the uncertainty in RM estimation, and in some cases even limits the estimation of RM (e.g., estimation for the burst shown in

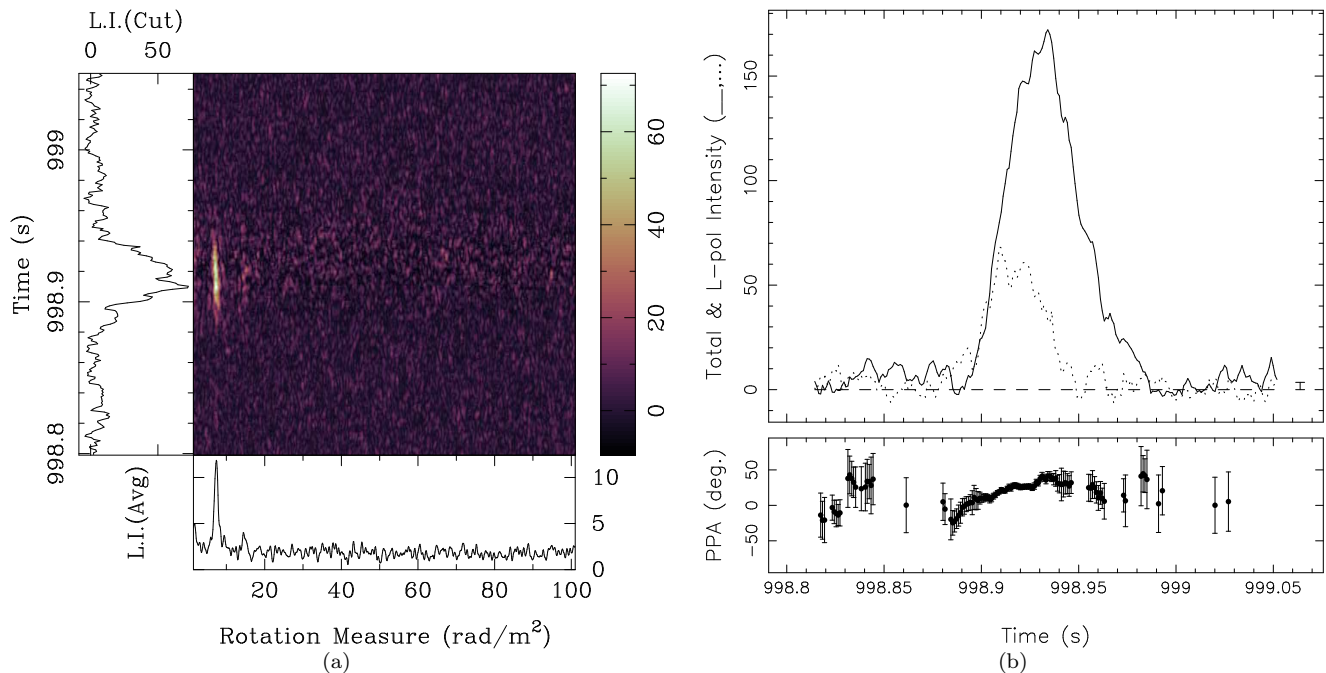


FIG. 2.— *Rotation measure synthesis and linear polarization properties of the burst shown in Figure 1(b)*: The central panel in subfigure (a) shows Faraday amplitude spectra (linearly polarized intensity as a function of RM) at different times around the burst location. The bottom and left panels show the average Faraday amplitude spectrum and a vertical cut across the maximum in the central panel, respectively. The upper panel in subfigure (b) shows the total (continuous line; in arbitrary units) and the linearly polarized intensity (dotted line; corresponding to $RM=7.3 \pm 0.4 \text{ rad m}^{-2}$) profiles of the burst. The lower panel shows the PPA behavior across the burst.

Figure 1(a) was not possible, although it seems consistent with a RM of about 10 rad m^{-2} . As mentioned earlier, estimation of RM is also limited by the S/N of individual samples. Despite these limitations, RM could be estimated unambiguously for 7 bursts discovered in session A, and these estimates³ are listed in Table 1. The linear polarization properties of these 7 bursts are shown in Figures 2(b) and 3.

3.3. Search for Transients toward Control Sources and Blank Sky

The control source observations were analyzed to detect periodic signals from the known pulsars and to search for any transient events. Average periodic signals as well as infrequent bright pulses from the control pulsars B0834+06 and B1919+21 were regularly detected at their corresponding DMs. On the day corresponding to session-A observations, both the control pulsars were observed. B1919+21 was observed about 11 hours before the session-A, while B0834+06 was observed about 2 hours after the session. Towards B1919+21, no genuine single pulse candidate was found above 8σ significance. B0834+06 observation was carried out in the afternoon (one of the peak times for RFI at the observatory), and was severely affected by RFI (much more than the session-A). Although such severe RFI

³ The RM estimates are obtained from a $(S/N)^2$ -weighted average of Faraday spectra across the pulses. However, the uncertainties mentioned in these RM estimates are those obtained from individual Faraday spectra. We mention these larger uncertainties to take in to account any effect of convolution of filter response or scintillation feature in the Fourier domain. The actual uncertainties could be better (i.e., smaller) by 50–80% of those mentioned here.

made the search for single pulses nearly impossible, a search and manual inspection involving thorough investigations of the dynamic-spectra did not result in detection of any genuine transient candidate in the RFI-free parts of data. Several other gamma-ray pulsars (J1732–3131, J1809–2332, J1836+5925, J2021+4026, J2055+2539, J2139+4716) were also observed on the same as well as the previous day of session-A observations. No significant dispersed pulse was found in these observations. Average periodic signal from both the pulsars (despite the severe RFI conditions during B0834+06 observation) could be detected at $\sim 10\sigma$ level, providing confidence in the system-health.

In the absence of any known radio pulsars or detection of signals from the target sources, our pointings towards all the gamma-ray pulsars effectively amount to observing the blank sky. Search for transient events in these blank sky observations (nearly 250 individual sessions of 30 minutes each) also did not result in detection of any significant dispersed pulse (Maan & Aswathappa 2014).

4. FAST RADIO TRANSIENTS: POSSIBLE SOURCE AND EMISSION MECHANISM

4.1. Source of the radio bursts

In the previous section, we presented discovery and properties of several fast radio transients with pulse widths in the range 30–270 ms. The radio bursts exhibit two important properties which are likely to be associated with their propagation through the ISM. Their times of arrival across the observation bandwidth closely follow the behavior expected from the cold-plasma dispersion relation, and several of the bursts also exhibit spectral intensity modulations that are likely to be due to differential Faraday rotation of the plane of linear po-

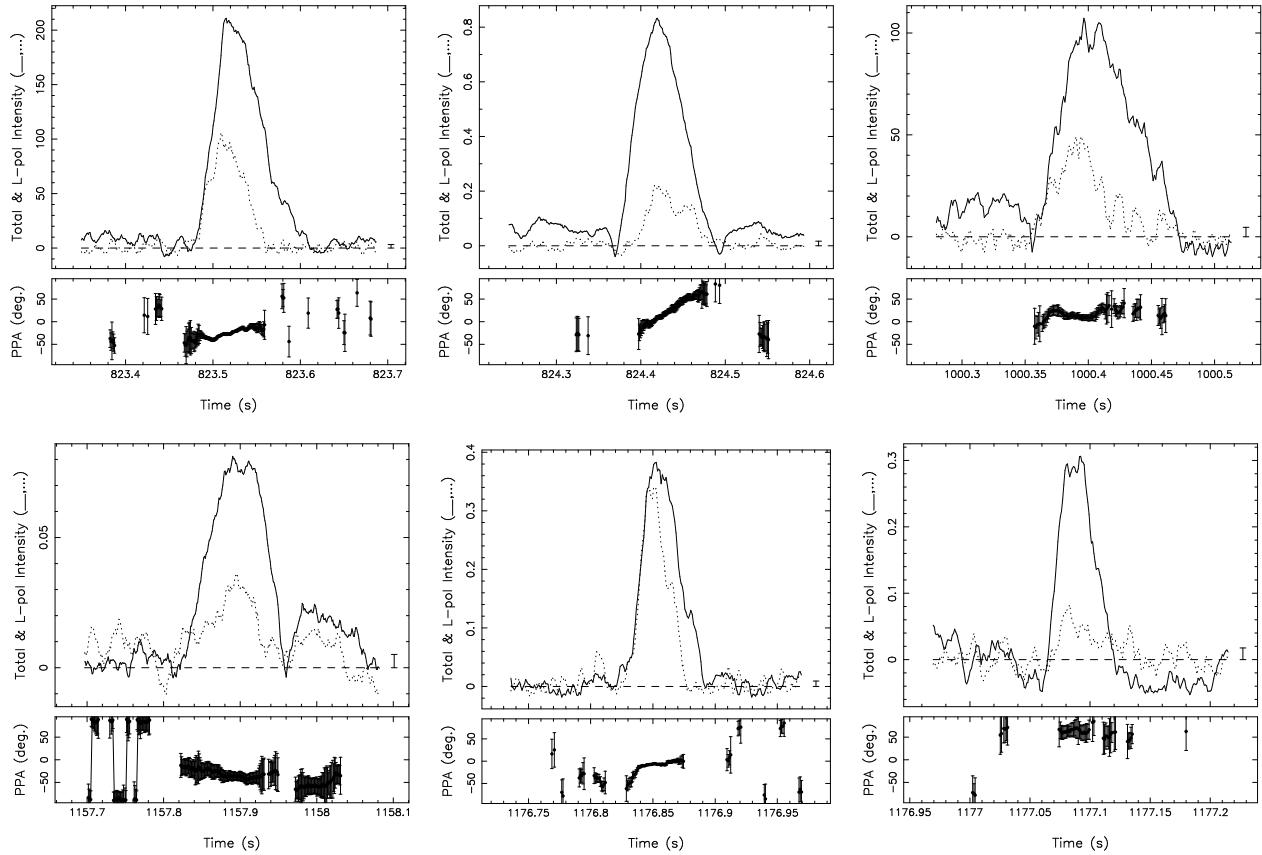


FIG. 3.— *Linear polarization profiles of radio bursts:* Linear polarization properties (continuous line: total intensity in arbitrary units, dotted line: linear polarization intensity, and PPA in the lower panels) of six radio bursts corresponding to their estimated RMs (see Table 1) are shown.

polarization within the observing bandwidth.

Sometimes, the swept-frequency RFI can mimic the dispersive signature of astronomically originated signals across the bandwidth. However, the times of arrival of a swept-frequency RFI are generally linearly proportional to the frequency, as against the ν^{-2} dependence in the dispersion relationship (Section 3). As a part of further critical assessment, data corresponding to the brightest radio burst (shown in Figure 1(a)) were dedispersed using linear delay gradients ($\Delta t \propto \nu$) spanning adequate delay ranges. The significance of detection in this case was found to be much lower compared to that obtained using the dispersion relation ($\Delta t \propto \text{DM} \nu^{-2}$), suggesting the signal to be of astronomical origin. Furthermore, several of the radio bursts also exhibit spectral modulation corresponding to the Faraday rotation in the intervening magneto-ionic medium. It would require a conspiracy for the swept-frequency RFI to mimic the dispersive as well as the Faraday rotation signature of astronomical signals. Note that the maximum ionospheric contribution towards RM, during the observing session A, is estimated⁴ to be only 2 rad m^{-2} — much smaller than RM of

⁴ The Earth’s ionosphere also contributes to the observed RM, and its contribution depends on the total electron content and the Earth’s magnetic field component along the line of sight. To estimate the amount of ionospheric Faraday rotation for the specific epoch, geographic location, and line-of-sight corresponding to our observations, we used the software *ionFR* (Sotomayor-Beltran et al. 2013, <http://sourceforge.net/projects/ionfr/>). *ionFR* uses the

various bursts ($6\text{--}10 \text{ rad m}^{-2}$). Hence, the deduced RM values also indicate the source of radio bursts to be much beyond the Earth’s ionosphere (i.e., at astronomical distances). Several of the radio bursts also show indications of an exponential tail in their pulse shapes (e.g., the bursts shown in Figure 1, that in top-left subplot of Figure 3, and a couple of bursts not shown) — a characteristic often associated with interstellar scattering of pulsed signals⁵. Non-detection of any transient events towards several other sky directions (see Section 3) also strongly supports the inference that the bursts could not have been a result of some man-made or system-originated signal. Hence, it is nearly certain that these radio bursts have their origin in an extraterrestrial source.

Although the estimated DMs of various radio bursts are not consistent with a single DM value, and lie in the range $1.4\text{--}3.6 \text{ pc cm}^{-3}$ (Table 1), it is unlikely that the bursts corresponding to different DMs originated from different radio sources that were coincidentally active only within the short spans of 2 observing sessions (A & B; out

International Geomagnetic Reference Field and a number of publicly available, GPS-derived total electron content maps. Since the telescope beam-width is very large ($\sim 25^\circ$) in declination, we examined several lines of sight within the beamwidth, and the maximum ionospheric RM was found to be 2 rad m^{-2} .

⁵ Large pulse-widths, spectral structures due to scintillation and Faraday rotation, and small amount of apparent scattering (as expected for the correspondingly small DMs), make it inadequate to test the power-law dependence of the scatter-broadening across the bandwidth.

of 130 sessions). The reason for variation in DM is more likely to be associated with the source or the intervening medium. With this argument, the following discussion proceeds with the assumption that all the radio bursts have been originated from a single astronomical source.

4.1.1. Could the bursts have originated from Sun ?

Type II/III solar bursts (see, for example, McLean & Labrum 1985) can sometime mimic the dispersive signature of distant astronomical pulsed signals. The spectral slopes or the frequency drift rate of these bursts depend on the plasma density and could vary from one burst to the other. However, widths of type III bursts are typically of the order of 1 s or more, and those of type II bursts are of the order of several minutes, i.e., much more than the widths of radio bursts under consideration. Furthermore, so far there is no evidence for solar radio bursts to have any significant linear polarization. Also, during the observing sessions A and B, Sun's position was about 15° away from the pointing RA (beamwidth in RA is $\approx 0.35^\circ$). Hence, bursts from Sun could have been detected only from a very far side-lobe, implying a huge attenuation in measured burst's power. These aspects, especially the observed narrow widths and significant linear polarization, make it unlikely that these bursts could have been originated from the Sun. To further explore any minor possibility of these bursts being associated with the Sun, we used the archived solar monitoring data from IZMIRAN's Solar Radio Laboratory⁶ (Gorgutsa et al. 2001) with a time resolution⁷ of 1 second. A part of these data corresponding to a bandwidth of about 1.5 MHz centered at 34 MHz were examined, and no event was found around the epochs of the radio bursts discovered in session A and B. An examination of archival solar monitoring data from the Learmonth and Culgoora observatories, albeit with a coarse resolution of 3 s, also did not indicate any event corresponding to the epochs of radio bursts under consideration. Hence, it is conclusive that these radio bursts have not originated from the Sun.

4.1.2. A pulsar as a possible source of radio bursts

Pulsars are known to emit bright radio pulses with high degree of linear polarization. Some pulsars also emit in the form of extremely bright and narrow pulses called giant-pulses. However, the observed short timescale variation in DM is unprecedented. Arrival times of individual bursts depend on their DM, and a typical uncertainty of 0.1 pc cm^{-3} in DM would imply a corresponding uncertainty of about 360 ms in arrival times. Hence, search for a periodic signal, as expected from a pulsar, across the observing session would not be adequate. Nevertheless, we performed blind periodicity searches around the DMs suggested by the bursts. Although no significant periodic signal was found in these blind searches, we can still examine if the bursts have originated from a known pulsar within the beam.

⁶ <http://www.izmiran.ru/stp/lars/>

⁷ Originally, these data were recorded with a finer resolution of 0.04 s. However, before archiving, the time resolution was coarsened to 1 s by taking an average over consecutive 25 samples.

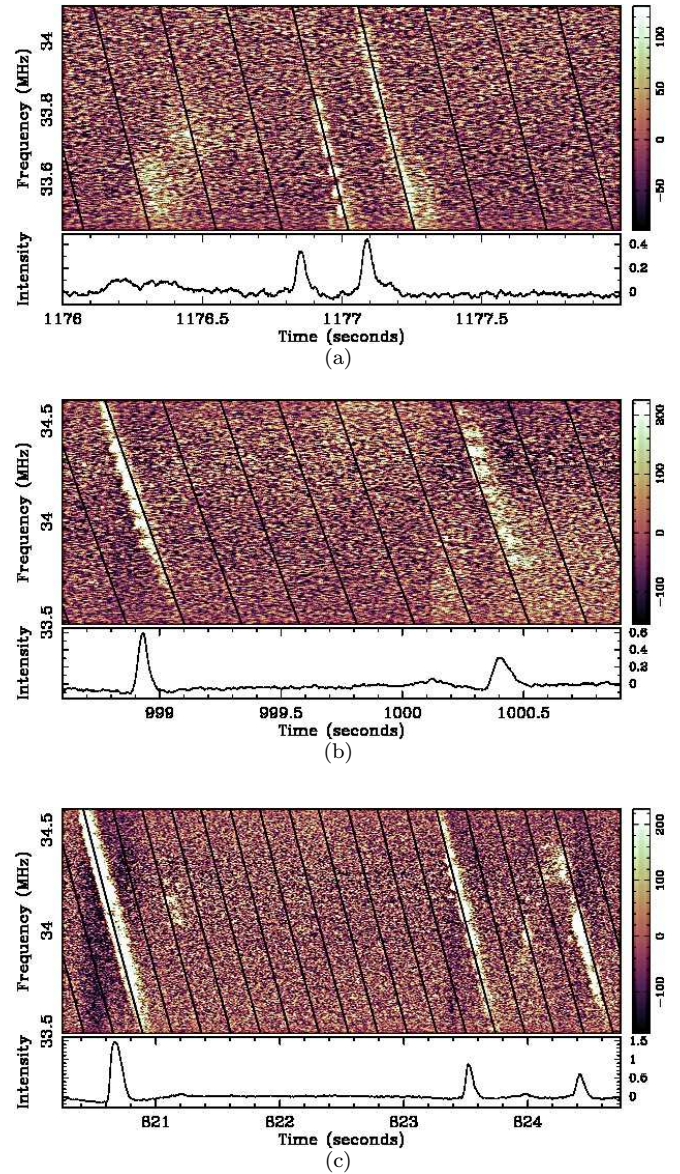


FIG. 4.— Spectrograms around groups of radio bursts: In each of the subfigures, the upper panel shows spectrogram around the selected group of bursts. The slanted thick black lines show the expected periodic times of arrival of radio pulses from Geminga pulsar when dispersed with DMs corresponding to that of bursts in subfigures (a), (b) and (c), i.e., 1.45, 2.05 and 1.40 pc cm^{-3} , respectively. The lower panels show the time series after the dispersion delays are corrected for a reference frequency of 34 MHz and using the above mentioned DMs. The spectrogram in (a) is limited to about 0.6 MHz (since the corresponding group of bursts do not extend beyond this bandwidth), while those in (b) and (c) are shown for parts of the bandwidth where the filter-response is nearly flat ($\sim 1.1 \text{ MHz}$).

The observations were originally targeted at the gamma-ray pulsars J0633+1746 and J0633+0632. To explore if the radio bursts have originated from one of these two pulsars, we note that there are groups of radio bursts which were detected within a few seconds duration and have DM as well as RM values consistent with each other. Three such groups comprise of burst numbers 1–3, 5–6, and 10–11 (hereafter, group A1, A2, and A3, respectively) in Table 1. Within each of these groups,

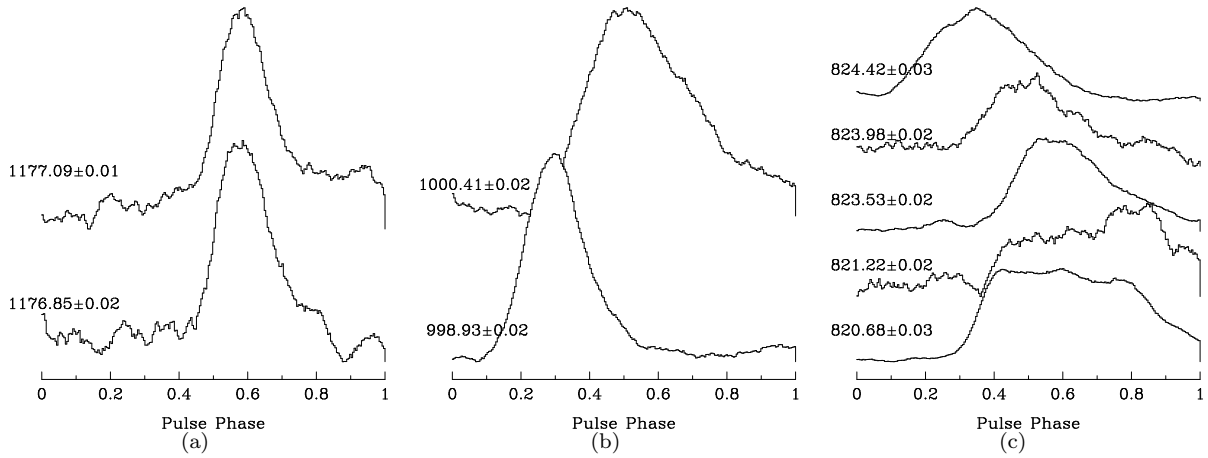


FIG. 5.— *Distribution of radio bursts in Geminga's rotation phase:* The panels (a), (b), and (c) show the bursts displayed in the spectrograms of Figure 4(a), 4(b), & 4(c), respectively, when dedispersed, and stacked according to their distribution in rotation phase of the pulsar. A small bandwidth of only 0.3 MHz (33.9–34.2 MHz) has been used for the bursts shown in panel (c), to avoid S/N-attenuation of the narrow band bursts. For each of the bursts, its arrival time (pulse-centroid in seconds; from start of observation) is shown on the left side.

we can examine if the arrival times of the bursts are consistent with the rotation period⁸ of either of the two pulsars. Figure 4 shows spectrograms (smoothed by a boxcar of width ~ 15 ms) around the above three groups of bursts, overlaid with expected arrival times of periodic pulses from Geminga pulsar (J0633+1746; rotation period ~ 0.237 s). The zero-phase of the expected periodic arrival times is different in the three spectrograms and, is chosen manually (since uncertainty in DM is inadequate for setting a common zero-phase). Figure 4(a) clearly suggests that the group A3 bursts (i.e., bursts 10 & 11) are consistent with being two consecutive radio pulses from Geminga pulsar, separated by just one rotation of the pulsar. Other 5 bursts in the remaining two groups (Figure 4(b) and 4(c)) are also consistent with them originated from Geminga pulsar and dispersed at the respective DMs of the burst-groups. Moreover, Figure 4(c) also shows additional, narrow-band signals at around 821.1 s and 824 s, which give rise to only hints of their presence in the time series. The arrival times of these narrow-band bursts, along with those of the other three strong and wider-band bursts, are also consistent with those expected from Geminga pulsar⁹. Arrival times of the two bursts in Figure 4(b) seem to be little offset from those expected from the pulsar, but still consistent within a phase-window of ~ 20 –25% of the pulsar's rotation period. Hence, arrival times of all the radio bursts within the three groups (5, 2 and 2 bursts in group A1, A2 and A3, respectively) strongly suggest that these bursts have originated from Geminga pulsar.

An examination of the distribution of dedispersed radio bursts in rotation phase of Geminga pulsar, separately for three burst-groups, gives a further clearer picture. As evident from Figure 5, first 4 bursts in group A1

(shown in panel (c)) and both the bursts in group A3 (shown in panel (a)) strongly suggest their origin to be Geminga pulsar. The pulse-profiles shown in Figure 5 are smoothed by a nearly 15 ms wide boxcar. The fourth burst (from bottom) in Figure 5(c) appears to be offset from the first three bursts by about 20 ms (nearly 10% of the pulsar period), however, given the effective resolution of about 15 ms and the uncertainty in pulse-centroid, this offset is not significant. Fifth burst in group A1 and the two bursts in group A2 are indeed slightly offset, however the observed offset of about 20% of the pulsar's rotation period is still comparable with the widths of the bursts. Malofeev & Malov (2000) have shown histograms of widths and arrival-phases of the average main and inter-pulse of Geminga. Their pulse-width ranges (about 20–140 ms and 0–90 ms, for main and inter-pulse, respectively), as well as the average phase-jitter range (about 0.2 of the period), are consistent with the respective parameters of the bursts presented here.

A similar examination of the spectrograms using the expected period of the gamma-ray pulsar J0633+0632 indicates that arrival times of only two pairs of bursts — 2,3 and 5,6 — seem to be consistent with the expected periodicity. However, note that the expected periods of Geminga and J0633+0632 at the epoch of our observation are about 0.2371 and 0.2974 s, respectively. Since the typical pulse-widths of the bursts under consideration are of the order of 50 ms or more, the two periods can have several common multiples where the arrival times of the bursts would appear to be consistent with both the periods. Indeed the above two pairs of bursts suffer from this ambiguity. However, the ambiguity is decisively resolved by the group A3 bursts, wherein the difference between the arrival times (220 ± 20 ms) clearly suggests the period to be consistent with that of Geminga pulsar.

Rotation periods of RRATs are generally derived by computing the largest common divisor of the differences between the burst arrival times at a given epoch (McLaughlin et al. 2006). This approach can also be applied to estimate any periodicity of the detected bursts independently. However, to ensure that the differences in arrival times are intrinsic to the source and not due to

⁸ The expected rotation period at the observation epoch is obtained by using the timing model provided by the LAT team at <https://confluence.slac.stanford.edu/display/GLAMCOG/LAT+Gamma-ray+Pulsar+Timing+Models> and the pulsar timing software TEMPO2 (<http://www.atnf.csiro.au/research/pulsar/tempo2/>).

⁹ Figure 4(a) also shows narrow-band signals between 1176.25–1176.5 s. Given their broad widths, comparing their arrival times with those expected from Geminga pulsar would not be adequate.

any variation in DM, the bursts only within the individual groups A1, A2 and A3 can be used for this purpose. Hence, we can use 4 independent arrival time differences — 2 differences from the arrival times of 3 wide-band bursts in group A1, and 1 each from the pairs of bursts in groups A2 and A3. A blind estimate of the period using these arrival time differences is 232 ± 8 ms, which is consistent with the rotation period of Geminga and further supports the above inference that the bursts have originated from Geminga pulsar.

To assess the chance probability of various bursts aligning with Geminga’s rotation phase, we performed Monte Carlo (MC) simulations for the three burst-groups. For group A3, it is significant that the two bursts appear to be consecutive pulses from the pulsar. To estimate the time-offset between the two bursts, brighter of the two pulses is used as a template and cross-correlated with the timeseries shown in Figure 4(a). From the cross-correlation function, the delay offset between the two bursts is estimated to be in the range 223–242 ms. An individual realization of MC simulation for this group involves generating two arrival times randomly and uniformly distributed within the observation duration of 1203 seconds. Using 10 million (10^7) such independent realizations, the chance probability of the two bursts occurring with the above mentioned delay is estimated to be 3.3×10^{-5} . In other words, the two bursts are consistent with being two consecutive pulses from Geminga pulsar at a confidence level of 99.997%.

For groups A1 and A2, the individual realizations of MC simulations consist of generating 5 and 2 bursts randomly distributed within time-extents of 5 and 2 seconds (as suggested by the durations within which these bursts have been observed; see Figure 4), respectively. Using 10 million independent realizations, the probability that the 5 bursts in group A1 could have aligned with each other within a phase-offset of ± 0.3 just by chance, is found to be 0.00922. Similarly, the chance probability of one burst in group A2 to be aligned with the other within a phase-offset of ± 0.4 is estimated to be 0.42851. Note that the above phase ranges sufficiently cover the phase-offsets¹⁰ between various bursts within the individual groups A1 and A2, as apparent from Figure 5. Moreover, by using the phase-offset ranges that extend on both sides of 0 (corresponding to perfect alignment), we have taken a liberal approach, i.e., both the possible signs of the relative offsets are allowed in the simulations. From the above chance probabilities, the confidence levels at which the bursts in groups A1 and A2 could be considered from Geminga pulsar, are 99.078% and 57.145%, respectively. The low confidence level for group A2 bursts to be associated with the pulsar has resulted due to (1) presence of only two pulses in the group which are also significantly offset from each other, and (2) our liberal approach in choosing the corresponding phase-offset range.

The net chance probability that the bursts in groups A1, A2 and A3 could have had the alignment with

Geminga’s rotation phase (within even the large offsets stated above), is only 1.3×10^{-7} ($0.00922 \times 0.42851 \times 3.3 \times 10^{-5}$). Hence, it is nearly certain, i.e., at a confidence level of 99.999987%, that the bursts have originated from the gamma-ray pulsar Geminga.

We also note that the distance to the source estimated using NE2001 model (Cordes & Lazio 2002) for the range of DMs sampled by various bursts in the two sessions is in the range 100–320 pc, which is consistent with the parallax distance to Geminga (250^{+120}_{-62} pc; Faherty et al. 2007).

Deep searches for persistent periodic signals from Geminga and J0633+0632 using all the observing sessions also improve the previous upper limits on respective flux densities (Maan & Aswathappa 2014) by a factor of about 1.5. The updated upper limits obtained by combining all the data are 25 and 19 mJy for Geminga and J0633+0632, respectively.

4.2. Possible emission mechanism of the radio bursts

The energies of the radio bursts are extremely high, and pulse-energies of this order have been observed to be emitted only from a handful of pulsars, in the form of giant pulses. The pulse energies of several radio bursts, including the brightest one, are comparable with those of the giant-pulses observed from Crab pulsar at decametre wavelengths (at 23 MHz; Popov et al. 2006). The comparable pulse energies suggest the radio bursts to be giant pulses from Geminga pulsar. The intrinsic widths of giant pulses have been observed to be very narrow — sometimes as small as a few nanoseconds (Hankins et al. 2003). Relatively larger widths of the bursts (30–270 ms) might have resulted intrinsically, or might have been caused by the same mechanism which is responsible for the short timescale variation in their DM. The giant pulse intensity and energy distributions exhibit power-law statistics (e.g., Argyle & Gower 1972), in contrast to those of the regular pulses which generally follow a normal distribution (e.g., Hesse & Wielebinski 1974). Given the statistically small number of bursts discovered in session A and B, pulse energy distribution is fitted equally well by power-law and normal distributions. Overall, the observed extreme pulse-energies might suggest the bursts to be radio giant pulses from Geminga pulsar.

4.3. Cause of variation in DM

The variations in DM of the bursts in session A take place at timescales¹¹ 55–160 s. The DM-range sampled by these bursts (1.4 – 2.6 pc cm^{−3}) corresponds to a maximum change of 0.005 cm^{−3} in the corresponding average electron density ($\langle n_e \rangle$) of the intervening medium across 250 pc. Such a change in ISM is possible, albeit only at very large timescales (of the order of years or decades). A larger change in electron density of a correspondingly smaller portion of the medium could be a more likely reason for the observed changes in DM. For example, if our sightline passes through a medium slab of thickness d_{pc} parsecs entirely responsible for the observed variation of 1.2 pc cm^{−3} in DM, then the required change

¹⁰ A correlation analysis similar to that performed for group A3 bursts, by using the brightest burst in the individual groups as a template and cross-correlating with the respective timeseries, was also performed for groups A1 and A2. The phase-offsets between various bursts suggested by this analysis are consistent within the phase-offset ranges we have used.

¹¹ Variations at shorter timescales are also apparent, but these are consistent with no-variation within 3σ error-bars, and hence, are less significant.

in electron density of this slab would be $1.2/d_{\text{pc}}$. Given the variation timescale and pulsar's transverse velocity of nearly 210 km s^{-1} , even a slab existing just next to the pulsar would imply appropriate thermal electron density variations to occur over extremely small spatial scales of just $\approx 10000 \text{ km}$ (i.e., $\sim 10^{-9} \text{ pc}$). Moreover, the required change in electron density at such a spatial scale would be of the order of 10^9 cm^{-3} . Such changes, at the required spatial scales, are unlikely to happen in the intervening medium even very near the pulsar, but might be possible within the pulsar magnetosphere. Possibility of a magnetospheric DM seems unlikely, although minor contribution of the magnetosphere towards the observed RM has not been excluded completely (Noutsos et al. 2009). Overall, the explanation for the observed short timescale change in DM would require a radically new theoretical approach, and detections of more bursts from the pulsar through extensive dedicated observations will help in obtaining more clues for the same.

5. DISCUSSION AND CONCLUSIONS

Radio emission from Geminga pulsar has remained puzzling, with comparable number of claims supporting the *radio-quiet* and *radio-loud* nature of the pulsar. Claimed detections of pulsed emission from the pulsar have been of low significance and the reported flux density appears to be highly variable. Even if the claimed detections are real, non-detections in several other sensitive searches suggest the radio emission from the pulsar to be non-persistent and variable. Although there has not been any other systematic search for transient emission from the pulsar, extensive searches have been conducted for periodic signal (e.g., Ershov 2007), and there has not been any precedence of detecting strong pulsed emission from the pulsar. Even in our 99 observing sessions, the bursts have been detected only in 2 sessions. Hence, the emission of such strong radio bursts from Geminga pulsar is a rare phenomenon.

Energies of the bursts compare well with those of the giant-pulses from the Crab pulsar at decametre wavelengths. The intrinsic widths of the giant pulses are known to be extremely narrow (nanoseconds to microseconds), compared to the moderately large widths (30–270 ms) of the bursts. Given the low DMs, the observed widths are unlikely to be associated with scattering in the intervening medium (in the thin screen approximation). However, the large widths might have contribution from the same mechanism that is responsible for the observed short timescale variation in DM.

Halpern & Ruderman (1993) have suggested that γ -ray emission from the outer-magnetosphere could produce copious e^\pm pairs in the inner-magnetosphere to quench Geminga's radio emission. They also note that for this quenching mechanism to work, a large inclination angle between the magnetic and rotation axis (so that a significant fraction of γ -rays pass through the inner-magnetosphere) is needed, and models of Geminga's gamma-ray emission indeed suggest a significantly inclined dipole (e.g., Zhang & Cheng 2001, estimate an inclination angle of $\sim 50^\circ$, and a viewing angle of $\sim 86^\circ$). On the basis of transient dips in Geminga's soft X-ray profile, Halpern & Wang (1997) suggest that the supply of copious e^\pm pairs in the inner-magnetosphere may be variable, and hence, occasional clearing away of the

quenching plasma might imply Geminga to be a transient radio emitter. If the claimed detections of radio emission from Geminga pulsar have indeed benefitted due to occasional ceasing of the quenching e^\pm pairs, detection of strong radio bursts might imply a complete cessation of the quenching plasma. Note that a small number of e^\pm pairs, e.g., just before cessation happens, might even help in triggering the creation of plasma pairs in the polar gap required for the radio emission process (Ruderman & Sutherland 1975). Dedicated observations of the pulsar simultaneously at radio frequencies and in X-rays can decisively find out if the above quenching mechanism is responsible for Geminga's radio quietness.

The short timescale variation in DM, if real, can also explain non-detection of periodic emission from Geminga pulsar in some of the earlier sensitive radio searches. Periodicity search crucially depends on the in-phase addition of pulsed signal. However, the variation in DM at timescales shorter than the integration time would imply a corresponding variation in arrival times of individual pulses. Hence, the short timescale variation in DM would make the periodicity search inadequate, and a search for a faint periodic signal using deep integration would be ineffective. However, note that the above effect is prominent only at lower frequencies ($\lesssim 150 \text{ MHz}$). Sensitive upper limits at higher radio frequencies together with detection of radio bursts presented here, and possibly the earlier claimed radio detections, indeed suggest Geminga pulsar to be radio-loud only occasionally.

Summarizing, we have presented discovery and detailed properties of several fast radio transients, with some of them highly linearly polarized, from the gamma-ray pulsar Geminga. These bursts exhibit variation in their dispersion measures (DM) over timescales as short as a minute, which is hard to explain by corresponding change in the electron density of the intervening medium. The short timescale variation in DM has remained the biggest puzzle in our findings. The energies of the bursts are comparable with those of giant pulses from Crab pulsar at decametre wavelengths, and might actually suggest the bursts to be radio giant pulses from Geminga. We have also discussed possibility of radio emission from Geminga due to occasional cessation of the copious quenching plasma in the pulsar's inner-magnetosphere (Halpern & Ruderman 1993; Halpern & Wang 1997). Detection of more bursts from the pulsar through dedicated low frequency observations can provide crucial clues to the underlying mechanism for occasional radio emission from Geminga, and possibly also from other radio-quiet gamma-ray pulsars. Discovery of these bursts have also demonstrated the potential of transient searches at very low frequencies.

ACKNOWLEDGMENTS

I thank the anonymous referee for a thorough review, and useful comments and suggestions. I am thankful to Aswathappa H. A. for help with the observations, and gratefully acknowledge the support from the observatory staff. The Gauribidanur radio telescope is jointly operated by the Raman Research Institute and the Indian Institute of Astrophysics. I am grateful to Roman Gorgutsa for providing archived solar monitoring data from IZMIRAN's solar radio laboratory (<http://www.izmiran.ru/stp/lars/>), and thankful to

Indrajit Barve for help in obtaining these data. Use of archived solar radio spectra provided by the Culgoora and Learmonth Solar Radio Observatories (Western Australia) has also been made, and I gratefully acknowledge Vasili Lobzin and Divya Oberoi for their help in obtaining these data. I am grateful to Harsha Raichur, Nishant Singh and Divya Oberoi for useful discussions and comments on the manuscript, and to Avinash A. Deshpande

and Bhal Chandra Joshi for useful suggestions at early stages of this work. Thanks are due to Arun K. Naidu, Bhal Chandra Joshi, P. K. Manoharan and M. A. Krishnakumar for providing the B0740–28 data acquired using the software backend of the Ooty radio telescope. I am thankful to the members of the LAT-team for providing the up-to-date timing models of several gamma-ray pulsars including Geminga.

REFERENCES

- Argyle, E., & Gower, J. F. R. 1972, *ApJL*, 175, L89
 Coenen, T. 2013, PhD thesis, Anton Pannekoek Instituut, Universiteit van Amsterdam, Amsterdam, The Netherlands
 Cordes, J. M., & Lazio, T. J. W. 2002, *ArXiv Astrophysics e-prints*
 Cordes J. M., & McLaughlin M. A., 2003, *ApJ*, 596, 1142
 Deshpande, A. A., Shevgaonkar, R. K., & Sastry, C. V. 1989, *J.IETE*, 35, 342
 Ershov, A. A. 2007, *ArXiv e-prints*
 Faherty, J., Walter, F. M., & Anderson, J. 2007, "Ap&SS", 308, 225
 Falcke, H., & Rezzolla, L. 2014, *A&A*, 562, A137
 Gorgutsa, R. V., Gnezdilov, A. A., Markeev, A. K., & Sobolev, D. E. 2001, *Astron. & Astrophys. Trans.*, 20, 547
 Gould, D. M., & Lyne, A. G. 1998, *MNRAS*, 301, 235
 Manchester, R. N., Han, J. L., & Qiao, G. J. 1998, *MNRAS*, 295, 280
 Halpern, J. P., & Ruderman, M. 1993, *ApJ*, 415, 286
 Halpern, J. P., & Wang, F. Y.-H. 1997, *ApJ*, 477, 905
 Hankins, T. H., Kern, J. S., Weatherall, J. C., & Eilek, J. A. 2003, *Nature*, 422, 141
 Hesse, K. H., & Wielebinski, R. 1974, *A&A*, 31, 409
 Hewish, A., Bell, S. J., Pilkington, J. D. H., Scott, P. F., & Collins, R. A. 1968, *Nature*, 217, 709
 Iwazaki, A. 2015, *Phys. Rev. D*, 91, 023008
 Kashiwayama, K., Ioka, K., & Mészáros, P. 2013, *ApJ Letters*, 776, L39
 Keane, E. F., Stappers, B. W., Kramer, M., & Lyne, A. G. 2012, *MNRAS*, 425, L71
 Kuz'min, A. D., & Losovskii, B. Y. 1997, *Astronomy Letters*, 23, 283
 Lorimer, D. R., Bailes, M., McLaughlin, M. A., Narkevic, D. J., & Crawford, F. 2007, *Science*, 318, 777
 Lyubarsky, Y. 2014, *MNRAS*, 442, L9
 Maan, Y. 2014, PhD thesis, Indian Institute of Science, Bangalore, India, <http://hdl.handle.net/2289/5908>
 Maan, Y., & Aswathappa, H. A. 2014, *MNRAS*, 445, 3221
 Maan, Y., Aswathappa, H. A., & Deshpande, A. A. 2012, *MNRAS*, 425, 2
 Malofeev, V. M., & Malov, O. I. 1997, *Nature*, 389, 697
 —. 2000, *Astronomy Reports*, 44, 45
 Malov, O. I., Malofeev, V. M., Teplykh, D. A., & Logvinenko, S. V. 2015, *Astronomy Reports*, 59, 183
 McLaughlin, M. A., Lyne, A. G., Lorimer, D. R., et al. 2006, *Nature*, 439, 817
 McLean, D. J., & Labrum, N. R. 1985, *Solar radiophysics: Studies of emission from the sun at metre wavelengths*
 Mottez, F., & Zarka, P. 2014, *A&A*, 569, A86
 Naidu, A., Joshi, B. C., Manoharan, P. K., & Krishnakumar, M. A. 2015, *Experimental Astronomy*, 39, 319
 Noutsos, A., Karastergiou, A., Kramer, M., Johnston, S., & Stappers, B. W. 2009, *MNRAS*, 396, 1559
 Noutsos, A., Sobey, C., Kondratiev, V. I., et al. 2015, *A&A*, 576, A62
 Popov, M. V., Kuz'min, A. D., Ul'yanov, O. M., et al. 2006, *Astronomy Reports*, 50, 562
 Popov, S. B., & Postnov, K. A. 2007, *ArXiv e-prints*
 Ramachandran, R., Deshpande, A. A., & Indrani, C. 1998, *A&A*, 339, 787
 Ramkumar, P. S., & Deshpande, A. A. 1999, *Journal of Astrophysics and Astronomy*, 20, 37
 Ruderman, M. A., & Sutherland, P. G. 1975, *ApJ*, 196, 51
 Seiradakis, J. H. 1992, *IAU Circ*, 5532, 1
 Shitov, Y. P., & Pugachev, V. D. 1998, *New Astronomy*, 3, 101
 Sotomayor-Beltran, C., Sobey, C., Hessels, J. W. T., et al. 2013, *A&A*, 552, A58
 Staelin, D. H., & Reifenstein, III, E. C. 1968, *Science*, 162, 1481
 Thornton, D., Stappers, B., Bailes, M., et al. 2013, *Science*, 341, 53
 Totani, T. 2013, *PASJ*, 65, L12
 Vats, H. O., Singal, A. K., Deshpande, M. R., et al. 1999, *MNRAS*, 302, L65
 Zhang, L., & Cheng, K. S. 2001, *MNRAS*, 320, 477